

**ERBIUM-DOPED FIBER RING LASER TUNING  
USING AN INTRA-CAVITY FABRY-PEROT FILTER**

A Thesis

by

**BILAL HAMEED MALIK**

Submitted to the Office of Graduate Studies of  
Texas A&M University  
in partial fulfillment of the requirements for the degree of

**MASTER OF SCIENCE**

August 2006

Major Subject: Electrical Engineering

**ERBIUM-DOPED FIBER RING LASER TUNING  
USING AN INTRA-CAVITY FABRY-PEROT FILTER**

A Thesis

by

**BILAL HAMEED MALIK**

Submitted to the Office of Graduate Studies of  
Texas A&M University  
in partial fulfillment of the requirements for the degree of

**MASTER OF SCIENCE**

Approved by:

Co-Chairs of Committee,	Chin B. Su Henry F. Taylor
Committee Members,	Christi K. Madsen Kuang-An Chang
Head of Department,	Costas Georghiadis

August 2006

Major Subject: Electrical Engineering

**ABSTRACT**

Erbium-Doped Fiber Ring Laser Tuning

Using an Intra-Cavity Fabry-Perot Filter. (August 2006)

Bilal Hameed Malik, B.S., Ghulam Ishaq Khan Institute of  
Engineering Sciences and Technology

Co-Chairs of Advisory Committee: Dr. Chin B. Su  
Dr. Henry F. Taylor

A tunable erbium-doped fiber ring laser using an intra-cavity Fabry-Perot filter as the tuning element is investigated. Tuning is achieved by varying the applied voltage which controls the FP cavity length. The laser's wavelength is monitored using an optical spectrum analyzer to determine the laser's spectral characteristics under static conditions at different wavelengths over its tuning range of approximately 50nm. When the laser is tuned rapidly, the frequency versus time characteristic is determined using a fiber Fabry-Perot interferometer with a photodetector to convert the optical signal to an electrical signal. The core of the research is to determine the degree of spectral broadening of the laser as a function of the spectral tuning rate. The fringe contrast of fiber Fabry-Perot interferometer transmittance curves decreases with increase in the tuning frequency. The gain at a certain wavelength becomes a function of time putting an upper limit on the tuning frequency of the system. The carrier lifetime of erbium ions dictates the maximum achievable tuning speed.

To My Parents

## ACKNOWLEDGMENTS

I would like to express my deepest gratitude and thanks to Dr. Henry F. Taylor (In memory of), co-chair of my advisory committee, for his guidance and counsel throughout my research process. I will always hold him in high esteem for the understanding and support he showed me during all times. I would also like to express sincere appreciation to Dr. Chin B. Su for his continuous support as co-chair of my advisory committee. I would like to thank Dr. Christi K. Madsen and Dr. Kuang-An Chang for serving as my committee members. Special thanks goes to Juan C. Juarez and Yang Ping for their helpful discussions.

## TABLE OF CONTENTS

	Page
ABSTRACT.....	iii
ACKNOWLEDGMENTS .....	v
TABLE OF CONTENTS.....	vi
LIST OF FIGURES .....	vii
LIST OF TABLES .....	ix
 CHAPTER	
I INTRODUCTION.....	1
II THEORETICAL BACKGROUND .....	4
A. Tunable Erbium-Doped Fiber Ring Lasers .....	4
1. Erbium-Doped Fiber Amplifier .....	5
2. Wavelength Division Multiplexers .....	7
3. Optical Isolators .....	9
B. Optical Filters .....	11
1. Tunable Fabry-Perot Filter.....	13
2. Fiber Fabry-Perot Sensor .....	13
III SYSTEM CONFIGURATION.....	15
A. Test Setup.....	15
B. Pump Laser Setup.....	18
IV EXPERIMENTAL RESULTS .....	20
A. Characterization of Ring Laser .....	20
B. Static Tuning of Ring Laser .....	26
C. Dynamic Tuning of Ring Laser.....	34
V CONCLUSION.....	40
VI RECOMMENDATIONS.....	42
REFERENCES .....	43
VITA.....	45

## LIST OF FIGURES

	Page
Fig.1. Multi-wavelength DFB laser arrays; SOA:Semiconductor Optical Amplifier [4].	2
Fig.2. Schematic of a tunable EDFRL .....	4
Fig.3. Schematic of an Erbium-Doped Fiber Amplifier .....	6
Fig.4. Wavelength selective coupling.....	8
Fig.5. Forward- and backward-propagating optical paths for a typical isolator design [13] .....	10
Fig.6. Fabry-Perot interferometer, with $P_i$ , $P_r$ , and $P_t$ the incident, reflected, and transmitted optical power, respectively. ....	11
Fig.7. Reflectance R as a function of the round trip phase shift for two individual mirror reflectance values, $R=0.9$ and $R=0.05$ . The quadrature points, halfway between the maximum and minimum reflectance points, represent the greatest sensitivity of reflectance to phase change.....	12
Fig.8. FFPI sensor with dielectric internal mirrors .....	14
Fig.9. Erbium-doped fiber ring laser setup .....	15
Fig.10. Signal tap output.....	16
Fig.11. The Fabry-Perot tunable filter (Photo courtesy Micron Optics).....	17
Fig.12. Block diagram of pump laser connections .....	18
Fig.13. Ring cavity - broken .....	20
Fig.14. Experimentally observed ASE spectrum.....	22
Fig.15. Theoretically modeled ASE spectrum.....	22
Fig.16. Ring cavity - complete.....	23

	Page
Fig.17. Ring laser output without filter.....	24
Fig.18. Tunable erbium-doped fiber ring laser .....	26
Fig.19. Graph – ring laser output as a function of pump laser power.....	28
Fig.20. Laser spectrum at voltage= 0.5 V.....	29
Fig.21. Laser spectrum at voltage= 1 V.....	30
Fig.22. Laser spectrum at voltage= 2 V.....	30
Fig.23. Laser spectrum at voltage= 3 V.....	31
Fig.24. Laser spectrum at voltage= 5 V.....	31
Fig.25. Laser spectrum at voltage= 7 V.....	32
Fig.26. Tuning – wavelength vs. applied voltage.....	33
Fig.27. FFPI transmittance – 0.1 Hz.....	35
Fig.28. FFPI transmittance – 0.5 Hz.....	35
Fig.29. FFPI transmittance – 5 Hz.....	36
Fig.30. FFPI transmittance – 50 Hz.....	36
Fig.31. Fringe visibility.....	38



**LIST OF TABLES**

	Page
Table 1. Pump Laser Output as a Function of Drive Current .....	21
Table 2. Summary: Broken Ring Cavity vs. Complete Ring Cavity .....	25
Table 3. Output Power vs. Drive Current .....	27

## CHAPTER I

### INTRODUCTION

For some time now, there has been a growing interest in optical communication in the low-attenuation wavelength range of 1.55  $\mu\text{m}$ . This is mainly due to two breakthroughs: wavelength division multiplexing (WDM), which is a method of sending many light beams of different wavelengths simultaneously down the core of an optical fiber; and the erbium-doped fiber amplifier (EDFA), which can amplify signals at many different wavelengths simultaneously, regardless of their modulation scheme or speed [1]. The channel spacing in the WDM systems has been diminishing due to constant increase in bandwidth demand and the limited gain range of the EDFA. This, in turn, requires increasingly accurate control and flexibility of an optical communication system to ensure reliable operation.

Lasers needed for WDM systems are much the same as lasers for ordinary long distance communication. However, some requirements like narrow linewidth and wavelength stability are more critical in WDM. One approach is use of multi-wavelength distributed feedback (DFB) laser arrays, where each laser operates at a particular wavelength. The output of these arrays can be joined together by a combiner element, like the one shown in Fig. 1. This makes it possible to couple the light from multiple lasers to a single optical fiber without the use of complicated external coupling optics [2]. However, the wavelength tuning capability of such devices is, in general, limited [3].

---

The journal model is *IEEE Photonics Technology Letters*.

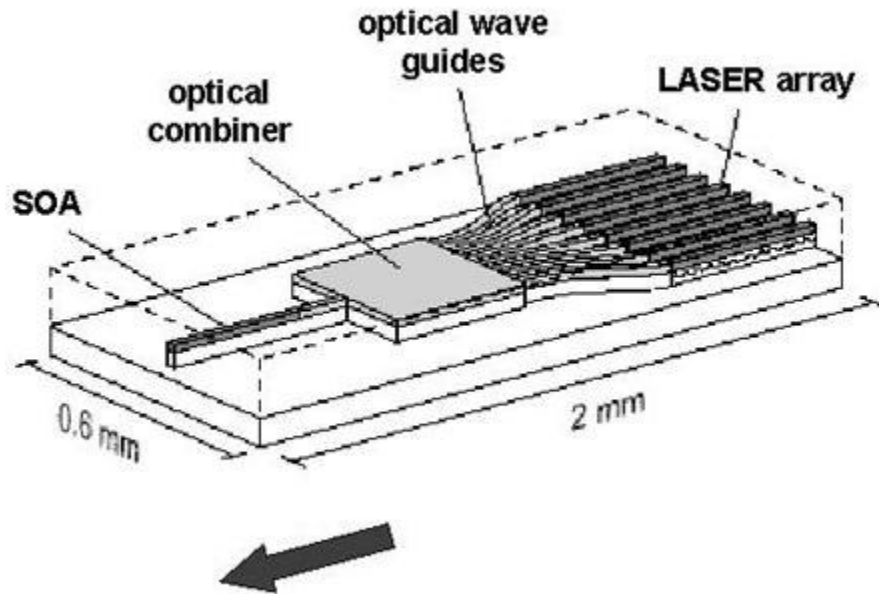


Fig.1. Multi-wavelength DFB laser arrays; SOA:Semiconductor Optical Amplifier [4]

Lately, lasers which are tunable over a broad spectrum of wavelength are gaining more significance. These devices are, in general, traditional semiconductor lasers that operate on same principles as their non-tunable counterparts. Most designs incorporate some form of corrugated layer which are similar to grating-like structure distributed Bragg reflector (DBR) or DFB configurations, but are much more complicated [5]. These structures can be dynamically altered in order to change the operating wavelength. This tuning is usually achieved by applying current to change the refractive index of the material, or by applying potential difference to change the physical dimensions of the gain medium or cavity.

In conjunction with readily available optical network elements like passive couplers and isolators, tunable laser technology can be reconfigured without the use of

such semiconductor lasers and other such devices. This, in turn, can lead to reasonable economic savings for all kind of optical communication networks.

In this thesis, a tunable erbium-doped fiber ring laser (EDFRL) is investigated. Tuning is achieved with the help of an intra-cavity Fabry-Perot (FP) optical filter. Voltage is applied to the filter which controls the effective cavity length of the ring laser. The optical output of the system is monitored using an optical spectrum analyzer (OSA). The tuning characteristics are determined through a fiber Fabry-Perot interferometer (FFPI) followed by a photo-receiver.

## CHAPTER II

### THEORETICAL BACKGROUND

#### A. Tunable Erbium-Doped Fiber Ring Lasers

A tunable erbium-doped fiber ring laser is shown in Fig. 2.

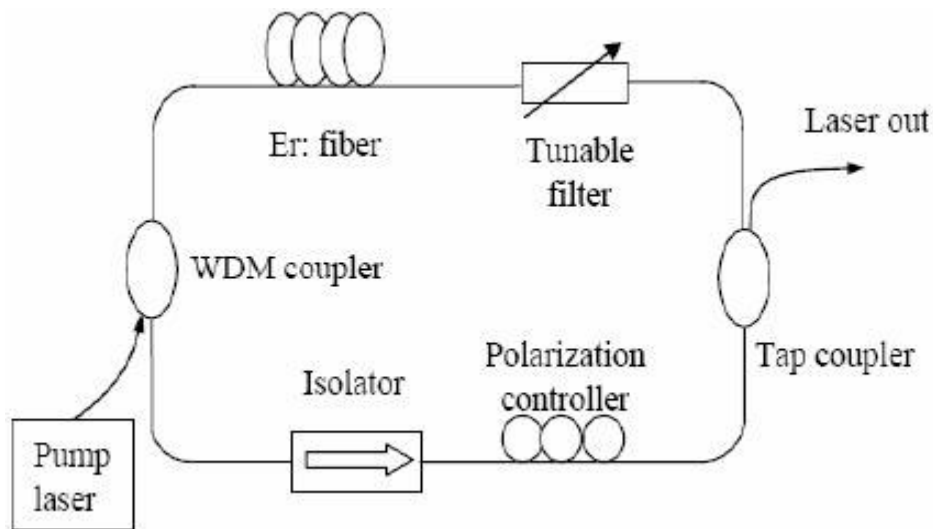


Fig.2. Schematic of a tunable EDFRL

The pump laser for erbium-doped fiber is usually a laser diode operating at wavelengths of 980 nm or 1480 nm, depending on the application. These wavelengths correspond to the absorption peaks of the erbium ions infused into the core of the fiber. The 980 nm band has a higher absorption cross-section and is generally used where low-noise performance is required. The 1480 nm band has a lower, but broader, absorption

cross-section and is generally used for higher power amplifiers. The pump laser output is coupled into the cavity by employing a wavelength division multiplexer. A polarization controller is incorporated to compensate for the birefringence of the fiber. An optical isolator in the circuit ensures that light only travels in desired direction. When operating in continuous mode, multiple longitudinal modes are anticipated [6-7]. To control the operation at a desired wavelength, an optical filter is integrated into the system. A tunable optical filter can make the system operate at any desired wavelength within the entire erbium-doped fiber gain spectrum. This spectrum includes both the *Conventional*, or C-band, from approximately 1525 nm – 1565 nm, and the *Long*, or L-band, from approximately 1570 nm – 1610 nm.

The major elements of an erbium-doped fiber ring laser design are as follows:

### **1. Erbium-Doped Fiber Amplifier**

Fiber amplifiers based on erbium-doped single mode fibers are widely used in long-haul optical fiber communication systems for compensating the loss of long fiber spans. An erbium-doped fiber amplifier (EDFA) consists of a short section of single mode fiber with controlled amount of rare earth element erbium doped to the core.

The principle involved here is similar to that of a laser. Erbium ions can exist in several electronic energy states: ground state and excited states. A photon of light can stimulate an electron in excited state to give away some of its energy, mostly in the form of a photon, and return to its stable ground state. This is called stimulated emission. The same electron can again be agitated to go into an excited state to again perform a stimulated emission.

As mentioned earlier, a laser diode at wavelengths of 980 nm or 1480 nm is used to pump the electrons into excited states. The energy associated with these wavelengths corresponds to the various excited states of erbium ions [8].

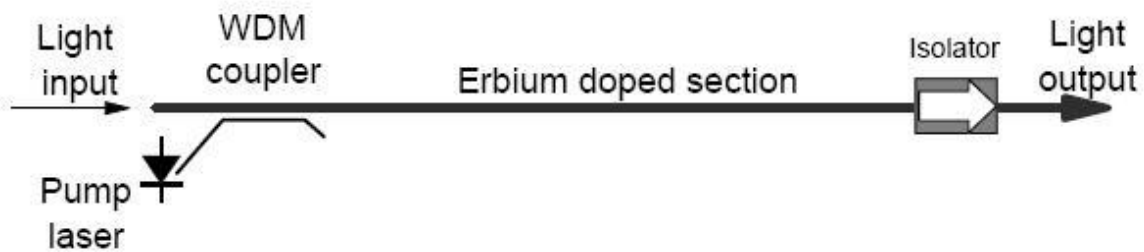


Fig.3.Schematic of an Erbium-Doped Fiber Amplifier

The basic operation of an EDFA, as illustrated in Fig. 3, is as follows:

1. A high power beam of pump laser is mixed combined with the input signal using a wavelength division multiplexer. The input signal is at a wavelength within the gain spectrum of the erbium-doped fiber.
2. The combination of pump and signal is then guided to a section of erbium-doped fiber.
3. The high power pump laser excites the erbium ions to go into higher energy (lower stability) states.

4. When the signal photons meet the energized erbium atoms, the erbium atoms give away some of their energy to the signal and return to the more stable lower energy state.
5. Amplification happens when erbium ions give up their energy in the form of photons which are coherent to the signal photons i.e. in phase and in the same direction as incoming signal photons. This way the signal is amplified only in the direction in which it is traveling. Thus all the additional power is guided in the same mode as the signal, and the system starts lasing.
6. An optical isolator is placed at the output to prevent reflections from the attached fiber and other connectors. These reflections tend to destabilize the laser.

The pump laser used in this research is a 980 nm laser diode. This provides a more complete conversion and highest level of inversion [9].

## **2. Wavelength Division Multiplexers**

Combining the signal and pump paths to allowing co-propagation and counter-propagation in the doped fiber region is provided by a wavelength division multiplexer (WDM). These couplers can also be used to split light into its constituent wavelengths. Fig. 4 shows how power transfer occurs in between the two inputs and one output [10]. The wavelength dependence of these couplers depends on the length of the coupling region. There are a number of design related characteristics are involved in manufacturing of these couplers. The most significant properties of these paths couplers



for signal and pump are the loss in both paths and the isolation i.e. how completely the two channels are separated.

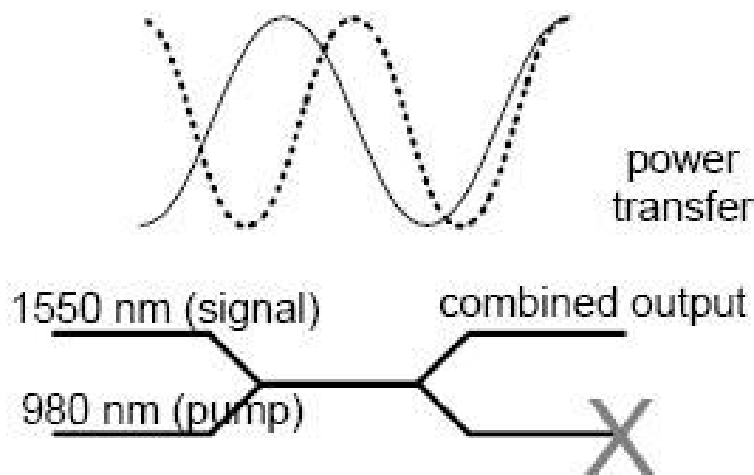


Fig.4.Wavelength selective coupling

In general, it may be necessary to combine several wavelength signal channels onto one fiber to make the most use of the available gain bandwidth of erbium-doped fiber. Such systems mostly need to combine  $N$  input wavelengths onto single output fiber or vice versa. Again, key to these systems are multiplexers that have low insertion loss for each channel and reasonable isolation. This can be achieved by various methods including arrayed waveguide gratings, fiber splitters, and optical filters.

### 3. Optical Isolators

Reflections at the input and output ports of an erbium-doped fiber laser may have a significant effect on its performance. These reflections may result from Fresnel reflections from connectors and components, or Rayleigh scattering from within the fiber [11]. Early designs of erbium-doped fiber lasers and amplifiers used oil-immersed fiber ends and angle-polished fiber ends to reduce the Fresnel reflections [1]. In general, reflections at the input end degrade the noise figure by reflecting the backward amplified spontaneous emissions. This in turn lowers the population inversion of the erbium ions [12].

Optical isolators are used in erbium-doped fiber laser systems to control the direction of propagation of light. An optical isolator is a device that allows light to pass in only one direction in the fiber. Its function in an optical system is similar to that of diode in the electrical world. Most optical phenomena are bi-directional and so building an isolator might be complicated. However, one optical phenomenon is not bi-directional. This is the Faraday Effect.

The Faraday effect is obtained when a magneto-optic material is placed in presence of a strong magnetic field. Light traveling within this material has its polarization state rotated by an amount depending on the length and strength of magnetic field. This is useful because the effect is asymmetric. The light traveling in one direction gets its polarization rotated by  $45^\circ$ . The light traveling in the opposite direction gets rotated in the same direction by same angle. So, effectively, light coming back into the input is at  $90^\circ$  to the original signal.

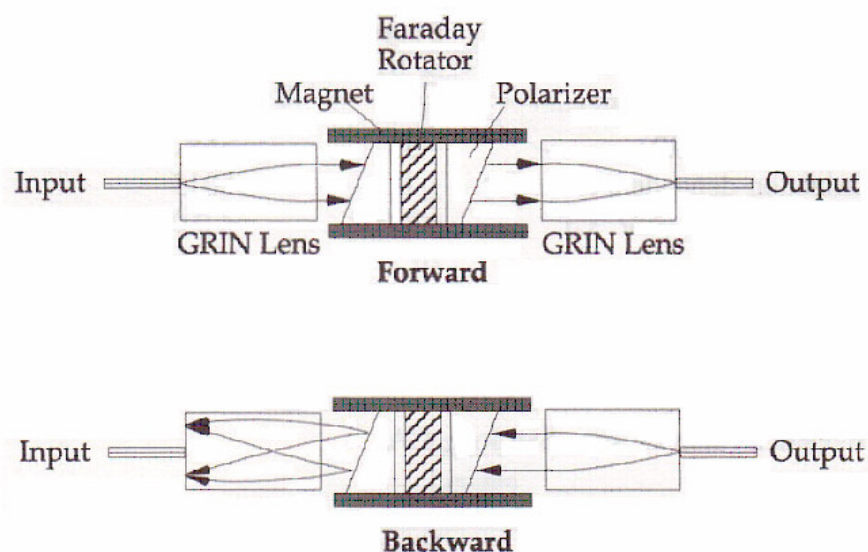


Fig.5. Forward- and backward-propagating optical paths for a typical isolator design [13]

The structure of a typical polarization-independent optical isolator is shown in Fig.5. Light traveling in the forward direction is collimated by the GRIN lens followed by a birefringent rutile wedge. The output of this wedge is then a pair of ordinary and extraordinary rays that pass through the Faraday rotator consisting of a length of magneto-optic material surrounded by a permanent magnet. This results in 45° rotation of the two polarization axes. These rotated rays then proceed through a second birefringent wedge which recombines them at the input of the output fiber. Backward-propagating light will experience first the separation into ordinary and extraordinary beams, rotated by the Faraday rotator to an angle now 90° from the input polarization, and sent on divergent paths by the second wedge. These different paths do not focus onto the input fiber and hence light is excluded from coupling back into the original optical path.

## B. Optical Filters

Erbium-doped fiber ring laser systems may use optical filters to enhance performance by suppressing amplified spontaneous emission and to select the operating wavelength. In this research thesis, a tunable filter is employed. Tunable filters provide flexibility in realization of useful erbium-doped fiber ring lasers.

Narrowband filters based on Fabry-Perot interferometers (FPI) are typically used to select the operating wavelength of the system. Fabry-Perot interferometer (FPI), sometimes called the Fabry-Perot etalon, consists of two mirrors of reflectance  $R_1$  and  $R_2$  separated by cavity of length  $L$  as in Fig. 6 [14].

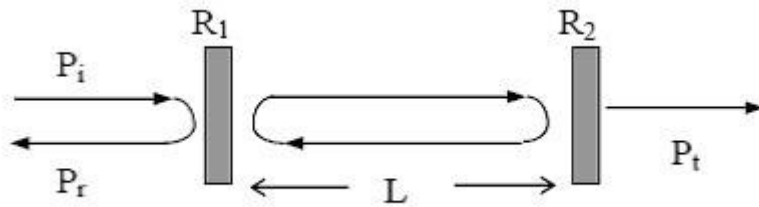


Fig.6. Fabry-Perot interferometer, with  $P_i$ ,  $P_r$ , and  $P_t$  the incident, reflected, and transmitted optical power, respectively.

The Fabry-Perot reflectance and transmittance are given by

$$R_{FP} = \frac{R_1 + R_2 + 2\sqrt{R_1 R_2} \cos \phi}{1 + R_1 R_2 + 2\sqrt{R_1 R_2} \cos \phi}, \quad (1)$$

$$T_{FP} = \frac{(1 - R_1)(1 - R_2)}{1 + R_1 R_2 + 2\sqrt{R_1 R_2} \cos \phi}, \quad (2)$$

where the round-trip propagation phase shift is given by

$$\phi = \frac{4\pi nL}{\lambda}, \quad (3)$$

with  $n$  the refractive index and  $\lambda$  the free space optical wavelength. It is evident from equation (1) that  $R_{FP}$  is maximum for  $\phi=2m\pi$ , with  $m$  an integer. In the case that  $R=R_1=R_2$ , with  $R \ll 1$ , then

$$R_{FP} \cong 2R(1 + \cos \phi), \quad (4)$$

$$T_{FP} \cong 1 - 2R(1 + \cos \phi) \quad (5)$$

According to equation (1), the reflectance is plotted as a function of phase shift in Fig.7 with  $R=0.9$  and  $R=0.05$ .

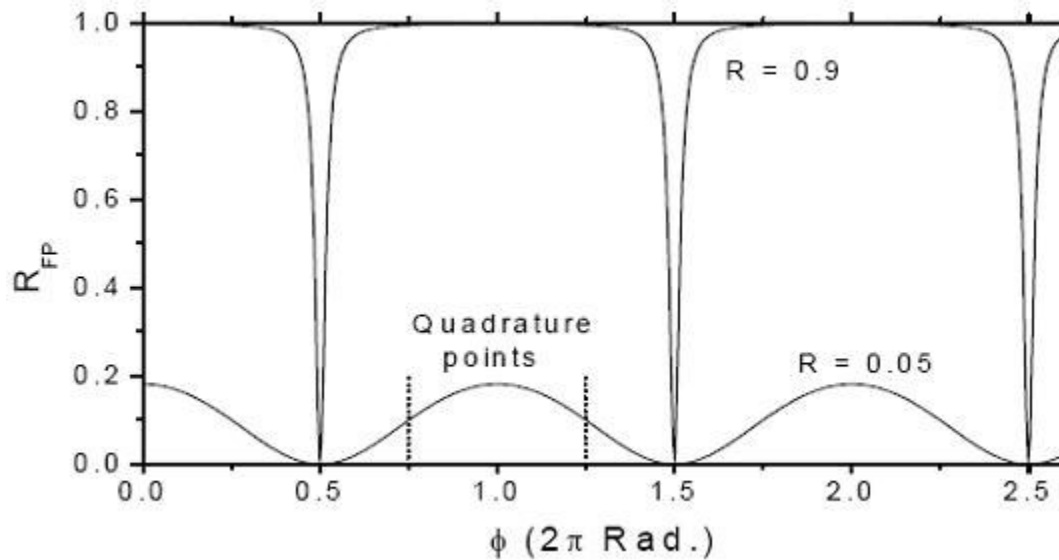


Fig. 7. Reflectance  $R$  as a function of the round trip phase shift for two individual mirror reflectance values,  $R=0.9$  and  $R=0.05$ . The quadrature points, halfway between the maximum and minimum reflectance points, represent the greatest sensitivity of reflectance to phase change.

## 1. Tunable Fabry-Perot Filter

It can be seen from equation (2) and (3) that, for  $R=R_1=R_2$ ,  $T_{FP}$  is approximately equal to 1, or  $(1-R \ll 1)$ , for certain values of  $\phi$ . Moreover  $\phi$  can be changed by changing the length  $L$  of the interferometer. This makes an interferometer to be used as a very high resolution optical filter. One of the ways to change the length of the etalon is that the interferometer is equipped with a high resolution mechanical positioning device, a piezoelectric transducer (PZT), to position the mirrors inside the etalon.

## 2. Fiber Fabry-Perot Sensor

As shown in Fig. 8, an intrinsic FFPI has two internal mirrors followed by a “non-reflecting” fiber end. The internal mirrors formed from dielectric coatings have shown good mechanical properties, low excess loss, and a wide range of reflectance. FFPIs are designed such that a measurand affects the optical length of the cavity, and light reflected or transmitted by the interferometer is converted by a photodetector to an electrical signal that is processed electronically to evaluate the measurand. The most commonly used mirror material is  $TiO_2$ , which has a refractive index of 2.4 (vs. 1.458 for fused silica). Thus the reflection results from refractive index discontinuities at the two film-fiber interfaces. A film  $\sim 100$  nm thick is deposited on the end of a fiber by electron beam evaporation. This fiber is then fusion spliced to the end of a second uncoated fiber. The fusion splicer is operated at lower arc current and duration than for a normal splice, and several splicing pulses are applied. The mirror reflectance generally decreases as a function of the number of splicing pulses, making it possible to select a desired reflectance over the range from  $\sim 1\%$  to about  $10\%$ . An excess loss of as low as  $1\%$  can

be achieved. Cavity lengths from  $100\ \mu\text{m}$  to  $1\ \text{m}$  have been demonstrated, with lengths in the vicinity of  $1\ \text{cm}$  commonly used.

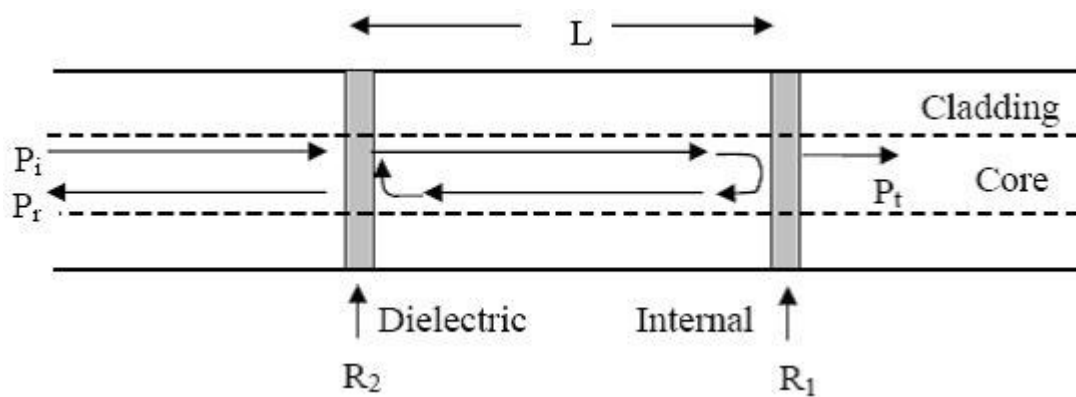


Fig. 8. FFPI sensor with dielectric internal mirrors

## CHAPTER III

### SYSTEM CONFIGURATION

#### A. Test Setup

The erbium-doped fiber ring laser system implemented in the laboratory is illustrated in Fig. 9.

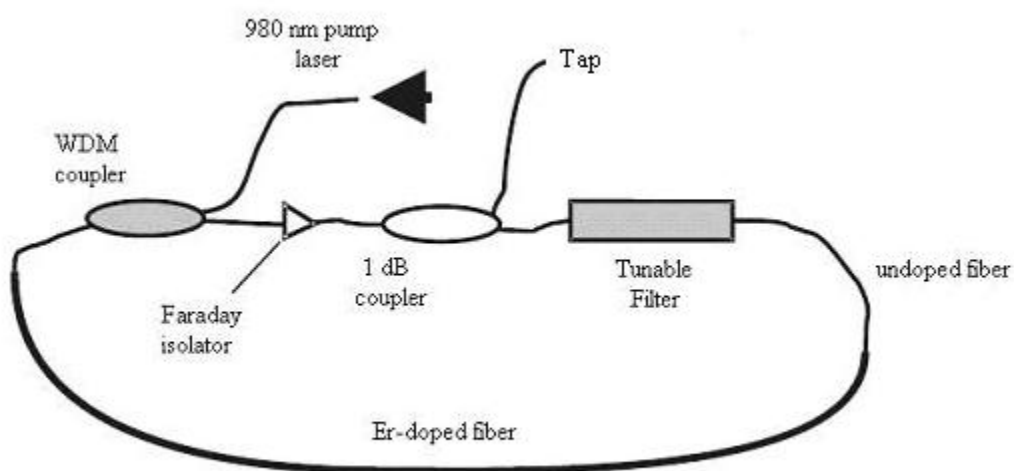


Fig. 9 Erbium-Doped Fiber Ring Laser Setup

The pump laser used in this setup is 980 nm. This in turn is coupled to a 6 m section of erbium-doped fiber, through a WDM coupler. The 1-dB couplers transmit 80% of the light in one arm and 20% in the other. The low output arm is used to tap out some



of the signal to study the static and dynamic tuning characteristics of this system. This output is then divided to observe the spectral and electrical characteristics separately (Fig.10).

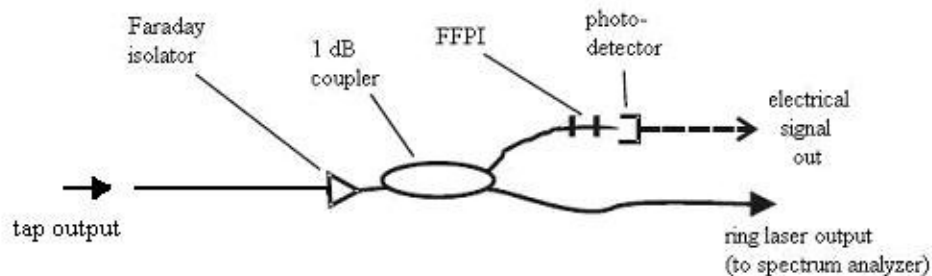


Fig. 10 Signal Tap Output

The tap output is further divided into two via another 1-dB coupler. The larger output is connected to an optical spectrum analyzer (OSA). The smaller output arm is connected to a FFPI which in turn is connected to a photodetector. An optical isolator is employed just before the optical filter to prevent any reflections and to preserve the direction of the light.

An optical filter is used to select the operating wavelength of the system. The filter used is a tunable Fabry-Perot filter, from Micron Optics (Fig.11). This new technology consists of adding a single segment of optical fiber within the original cavity of the filter. The high optical resolution of the novel device is maintained, but with a few significant properties:

- The optical filter has fiber attached to both sides of the cavity. This makes it more compatible to use in an all fiber system such as this setup.
- Unlike the original design, the light is guided within the fiber. The etalon guides the light with each bounce between the mirrors.
- The device is equipped with a high resolution mechanical movement device. This is a piezoelectric transducer (PZT) used to position the mirrors which constitute the cavity.

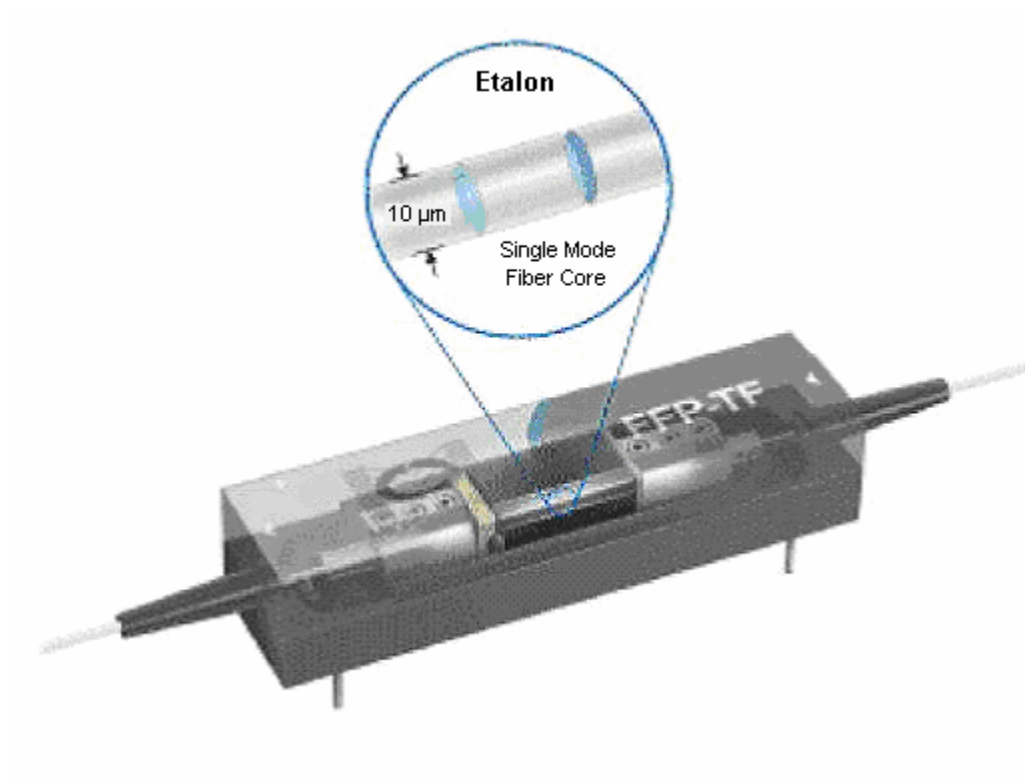


Fig.11 The Fabry-Perot Tunable Filter (Photo courtesy Micron Optics)

The filter passes select wavelengths that are equal to multiples of  $L/2c$ , where  $L$  is the length of the fiber cavity, and  $c$  is the free space velocity of light. The wavelength can be selected by applying voltage to the PZT, thus allowing tuning over a wide spectral range. The filter used here has insertion loss of about 3.5 dB.

### B. Pump Laser Setup

The setup for pump laser used to excite erbium-doped fiber is shown in Fig.12. Power supply for the thermo electric cooler is a constant 10 V source. The laser can be supplied up to 200 mA of driving current. The direction of propagation of pump laser is opposite to that of the signal.

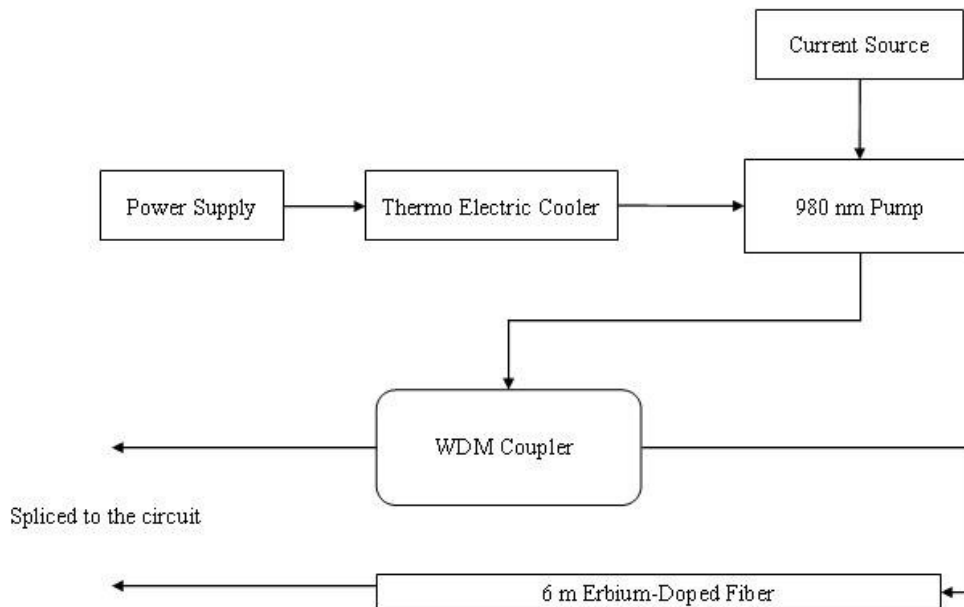


Fig.12 Block Diagram of Pump Laser Connections

Each of the described components has insertion loss associated with it. These are approximately:

- WDM Coupler: 1 dB
- 1-dB coupler: 1 dB
- Optical isolator: 1 dB
- Tunable optical filter: 3.5 dB

Adding these values, the total cavity loss incurred is expected to be 6.5 dB. The meter section of erbium-doped fiber has a maximum gain of 30 dB.

## CHAPTER IV

### EXPERIMENTAL RESULTS

#### A. Characterization of Ring Laser

This chapter gives the experimental results and observations taken during the course of characterizing and testing the laser. A spectrum analyzer is used to measure the spectral characteristics of the system. This includes the power and linewidth of the lasing wavelength.

The line of experiments starts first by breaking the loop of the ring laser and then connecting one of the ends to the spectrum analyzer.

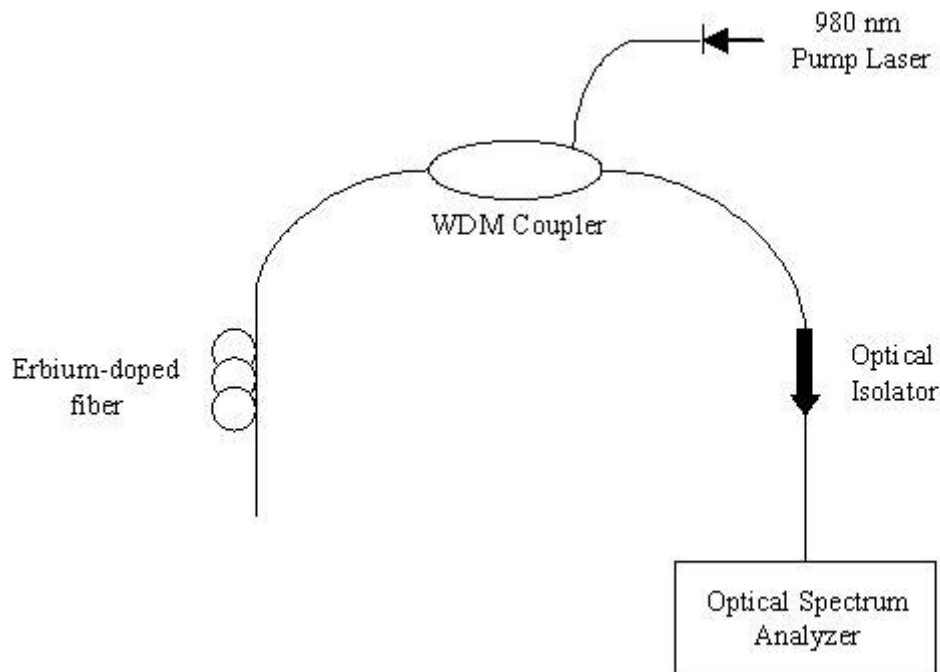


Fig. 13. Ring Cavity - Broken

The pump used in this system is a 980 nm laser diode. The pump power as a function of drive current is given in Table 1. Most of the experiments carried on this research were done with drive current of 100 mA which corresponds to pump power output of 47 mW.

Table 1. Pump Laser Output as a Function of Drive Current

<b>Drive Current (mA)</b>	<b>Pump Laser Output (mW)</b>
20	0
37	10
60	15
80	36
100	47
120	57
140	71
160	82
180	97
200	112

As shown in Fig. 13, the broken ring has no filter in the setup. Without the filter, the spectrum analyzer shows the spontaneous emission of the erbium-doped fiber. This is a characteristic of all erbium-doped fiber systems, and is called amplified spontaneous emission (ASE) profile of the system. The output ASE of this system is shown in Fig. 14. The spectrum has a peak at wavelength of 1531.1 nm and linewidth of 4.6 nm. This peak wavelength is in close agreement with the theoretical profile of erbium-doped fiber systems (Fig. 15).

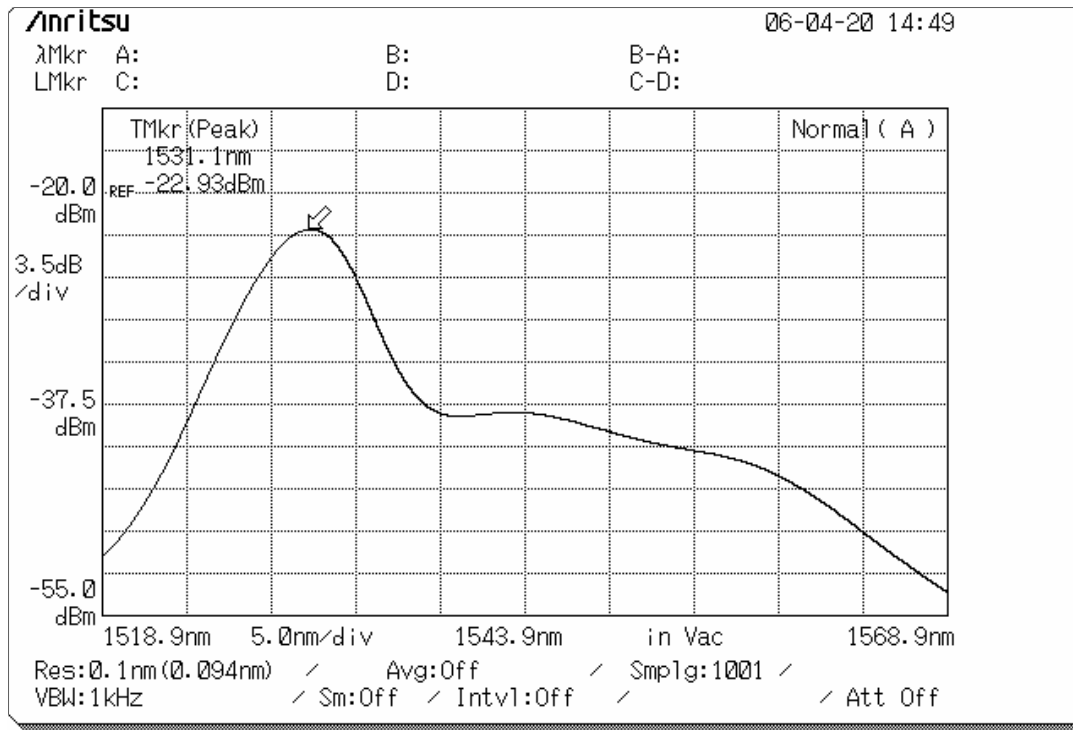


Fig. 14. Experimentally observed ASE spectrum

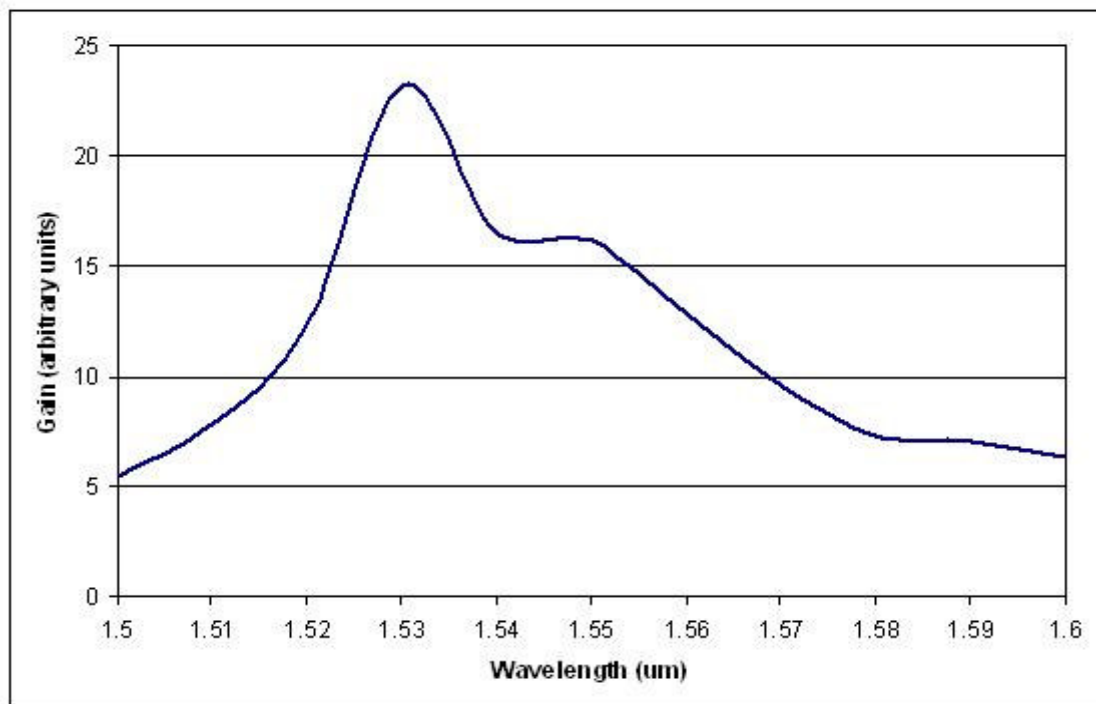


Fig. 15. Theoretically modeled ASE spectrum

The ring is completed by inserting a fiber coupler into the system (Fig.16). The input port of the coupler is connected to the output of the isolator. One of the output ports of the coupler is spliced to the free end of the erbium-doped fiber. Now the feedback loop is completed and the ring cavity starts lasing. The range of the spectrum analyzer is from 1200 nm to 1700 nm therefore it does not detect any light near pump laser wavelength of 980 nm. In addition, the direction of propagation of pump laser is opposite to that of the signal. Hence most of the pump laser power is absorbed by the erbium-doped fiber. The isolator in the circuit also helps to remove any unabsorbed pump light out of the system.

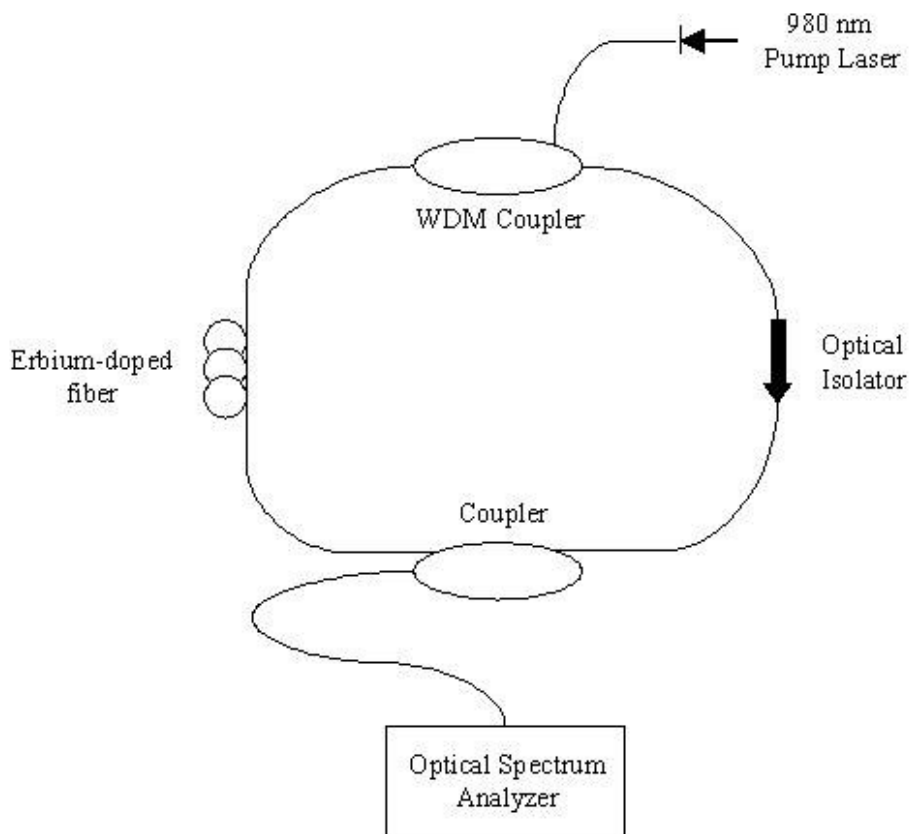


Fig. 16. Ring Cavity - Complete



The light signal detected by the spectrum analyzer is shown in Fig.17. The ring is now a laser emitting at 1530.17 nm with a linewidth of 0.053 nm; the linewidth being the spectral width where the laser power drops by 3 dB. At this point, the laser is actually lasing at a number of longitudinal modes. Due to long length of the cavity, these individual modes have very narrow linewidths. The detection of these modes is limited by the resolution of the spectrum analyzer, which is 0.05 nm. In effect, what we see is one peak which has a linewidth near to the resolution of the spectrum analyzer.

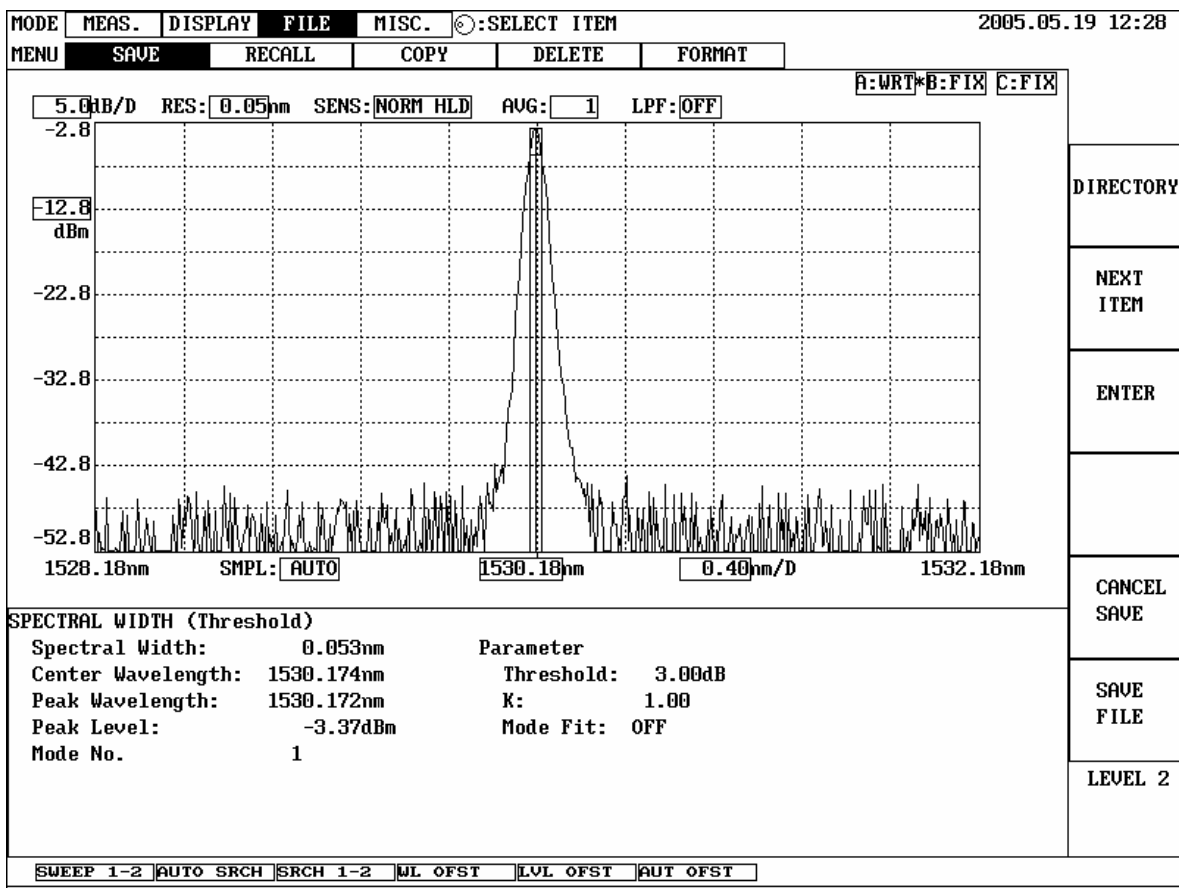


Fig. 17. Ring Laser Output without Filter

The peak output power is much higher when the ring is complete, reason being that light is now lasing. The peak wavelength of the laser output corresponds to the peak wavelength of the ASE spectrum of the erbium doped fiber. The ASE actually behaves as the gain spectrum of the laser. So when lasing starts, the modes of ring cavity near the peak of ASE gain much more amplification. The linewidth now is much narrower and the output power increases due to amplification. Also the side lobe suppression is increased in the case of the laser. The summary of these characteristics is given in Table 2.

Table 2. Summary: Broken Ring Cavity vs. Complete Ring Cavity

	<b>Peak Wavelength (nm)</b>	<b>Linewidth (nm)</b>	<b>Peak Output Power (dBm)</b>	<b>Side Lobe Suppression (dB)</b>
<b>Broken Ring Cavity</b>	1531.1	4.6	-22.93	> 10
<b>Complete Ring Cavity</b>	1530.17	0.053	-3.37	> 35

## B. Static Tuning of Ring Laser

In the next step, the tunable Fabry-Perot filter is added to the ring of Fig. 16. The use of this filter is to essentially determine the lasing wavelength of the system. It is added such that the output of the already present fiber coupler is connected to the input of the filter and the other end is spliced to the erbium-doped fiber (Fig. 18). Another isolator is added outside the cavity to prevent any reflections from measuring devices. The output coupler following this isolator divides the output into two. One goes to the spectrum analyzer or a power meter, to measure the spectral characteristics and optical power of the tunable ring laser, respectively. The other output is connected to a photodetector via a FFPI.

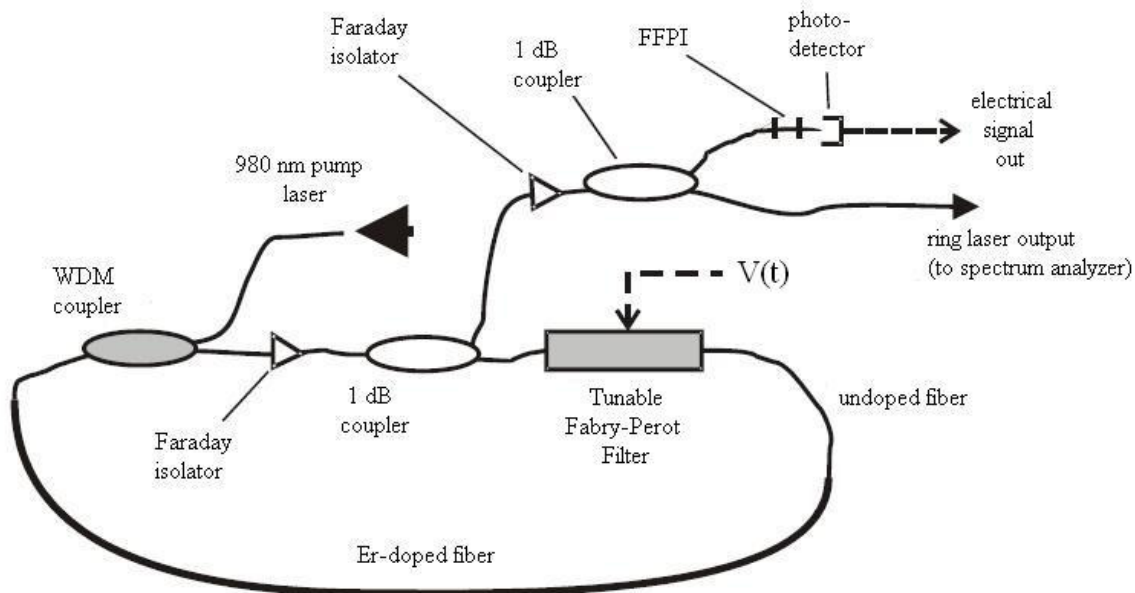


Fig. 18. Tunable Erbium-Doped Fiber Ring Laser

The output of the system is first connected to a power meter to characterize the laser power as a function of pump power. In general, there is always a certain threshold pump power and slope efficiency associated to optically pumped laser systems. The slope efficiency is the number of milliwatts or microwatts of light output per milliampere of increased drive current above threshold. Table 3 shows ring laser output power as a function a drive current.

Table 3. Output Power vs. Drive Current

<b>Drive Current (mA)</b>	<b>Ring Laser Output Power (mW)</b>
37	$1.0 \times 10^{-5}$
60	0.51
80	1.75
100	2.82
120	3.64
140	5.11
160	6.51
180	8.20
200	10.13

The threshold current for this system is approximately 37 mA. This corresponds to pump power of 10 mW. Once above the threshold current, the laser output power increases quite linearly as a function of pump power. This can be seen in Fig.19. The slope efficiency comes out be around 0.07 mW/mA.

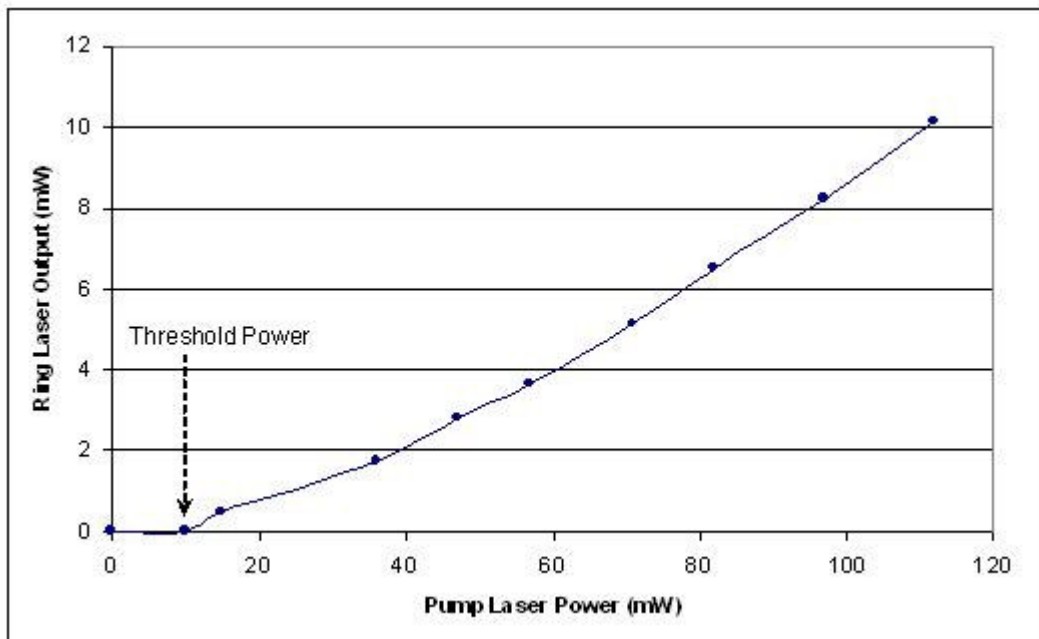


Fig. 19. Graph – Ring Laser Output as a function of Pump Laser Power

The end connected to the optical power meter is now connected to the spectrum analyzer. The electrical terminals of the tunable Fabry-Perot filter are connected to a variable DC power supply. The voltage is varied manually from 0 V to 7 V. The output spectrum of the ring laser system is observed and recorded with the help of the spectrum analyzer. At zero voltage, the laser operates at 1539.26 nm. As the voltage is gradually increased, the operating wavelength starts to increase. Various tests have been carried out at different supply voltage to the tunable Fabry-Perot filter. The output is recorded at these different voltage values varying from 0.5 V to 7 V, and is shown in Fig.20 through Fig.25.

The free spectral range of the tunable Fabry-Perot filter corresponds to 7 V. After 7 V, the filter jumps to another transmittance peak and the operating wavelength of the

laser goes shifts to the beginning of the wavelength cycle. The maximum input voltage this filter can handle is 70 V. The wavelength cycle keeps on repeating every 7 V.

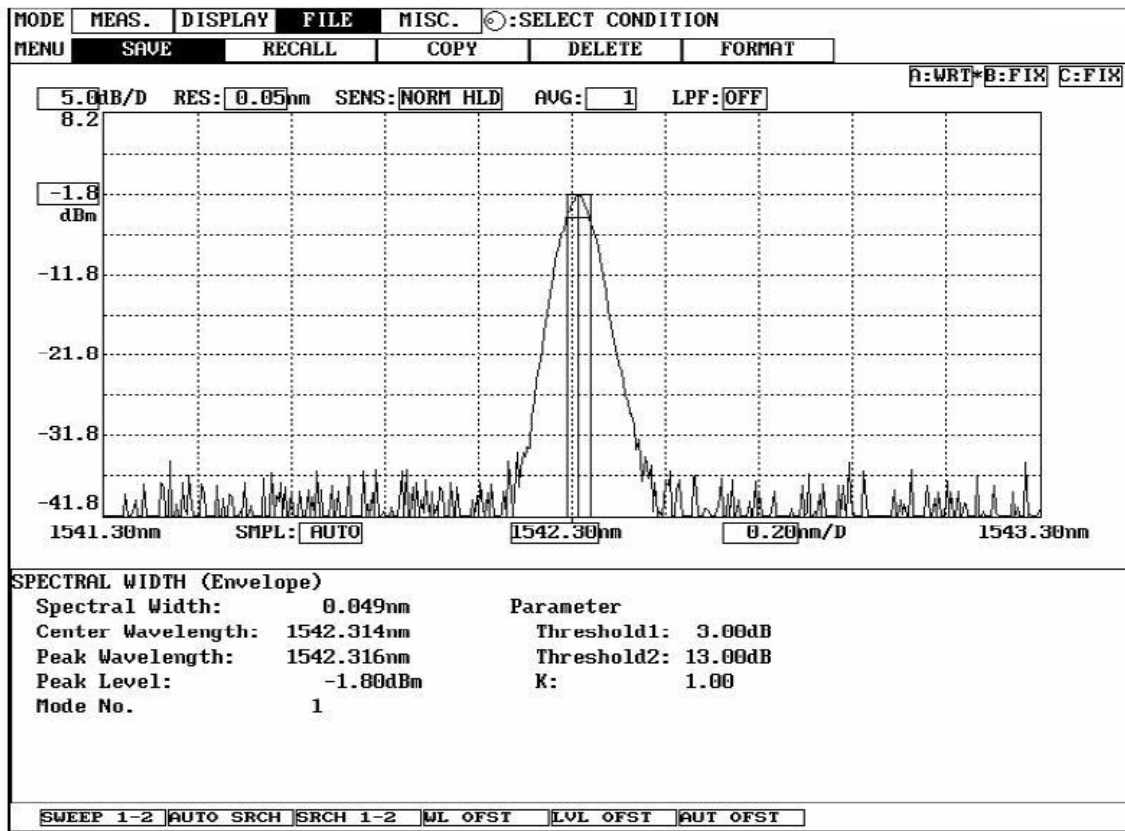


Fig. 20. Laser Spectrum at Voltage= 0.5 V

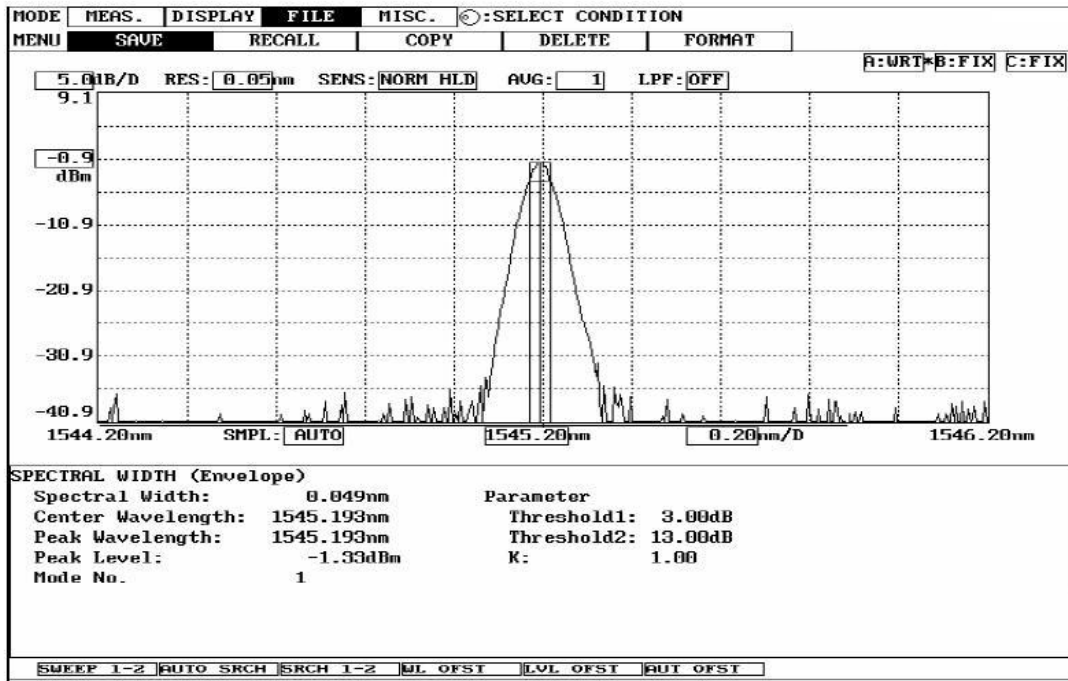


Fig. 21. Laser Spectrum at Voltage= 1 V

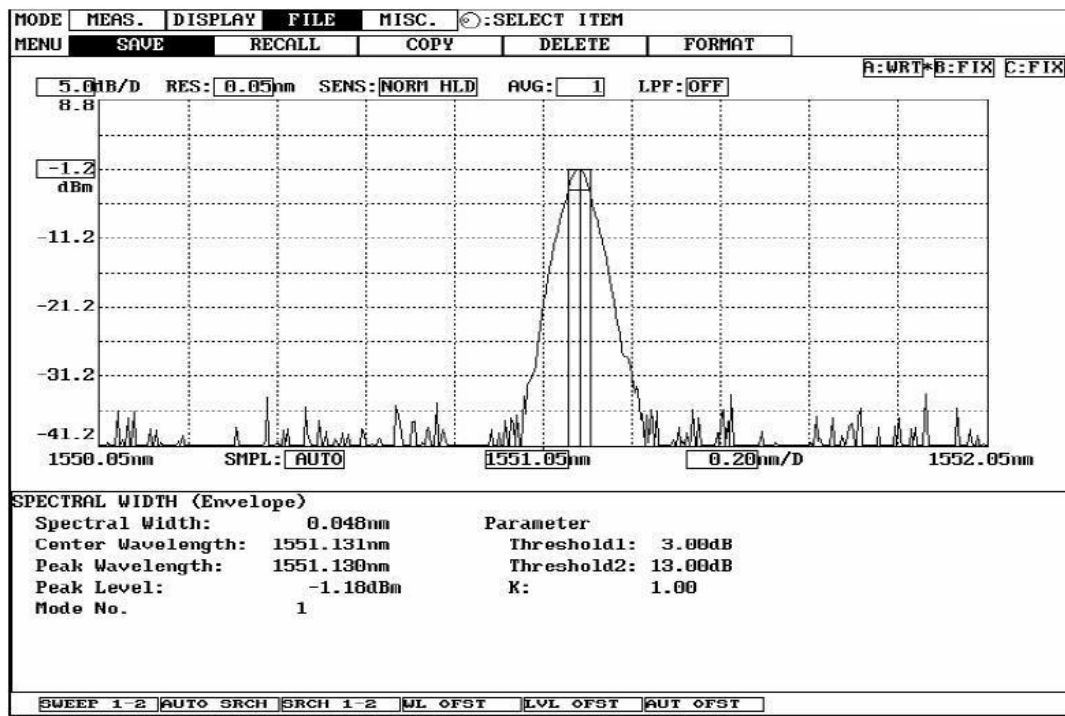


Fig. 22. Laser Spectrum at Voltage= 2 V

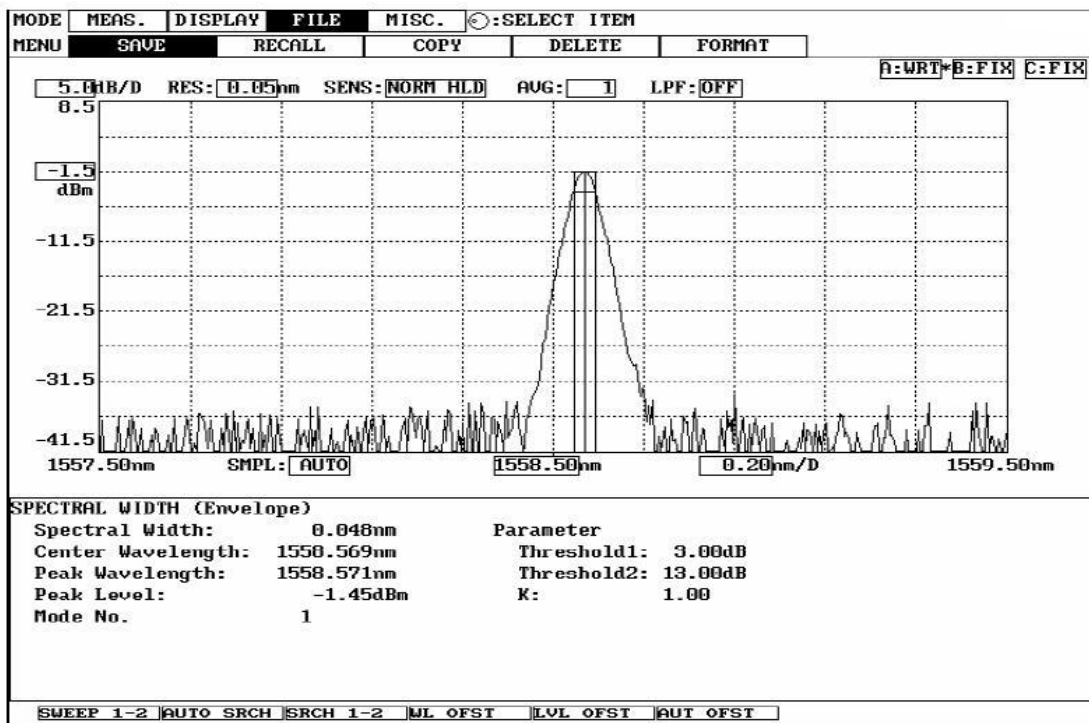


Fig. 23. Laser Spectrum at Voltage= 3 V

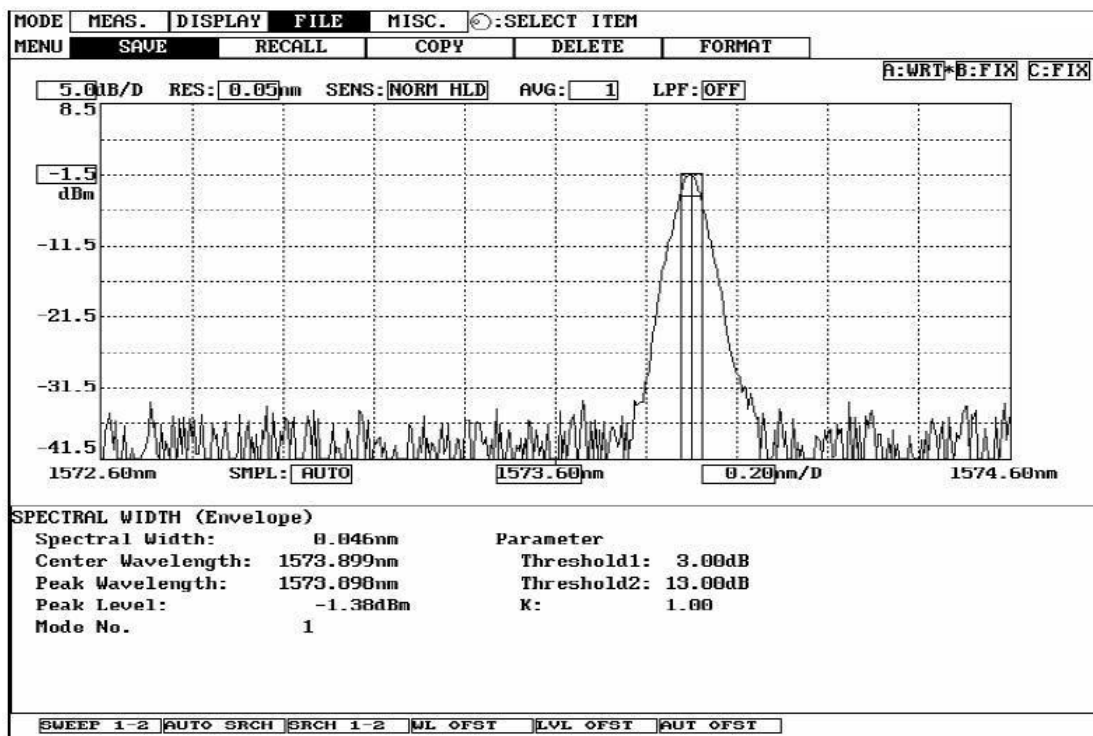


Fig. 24. Laser Spectrum at Voltage= 5 V



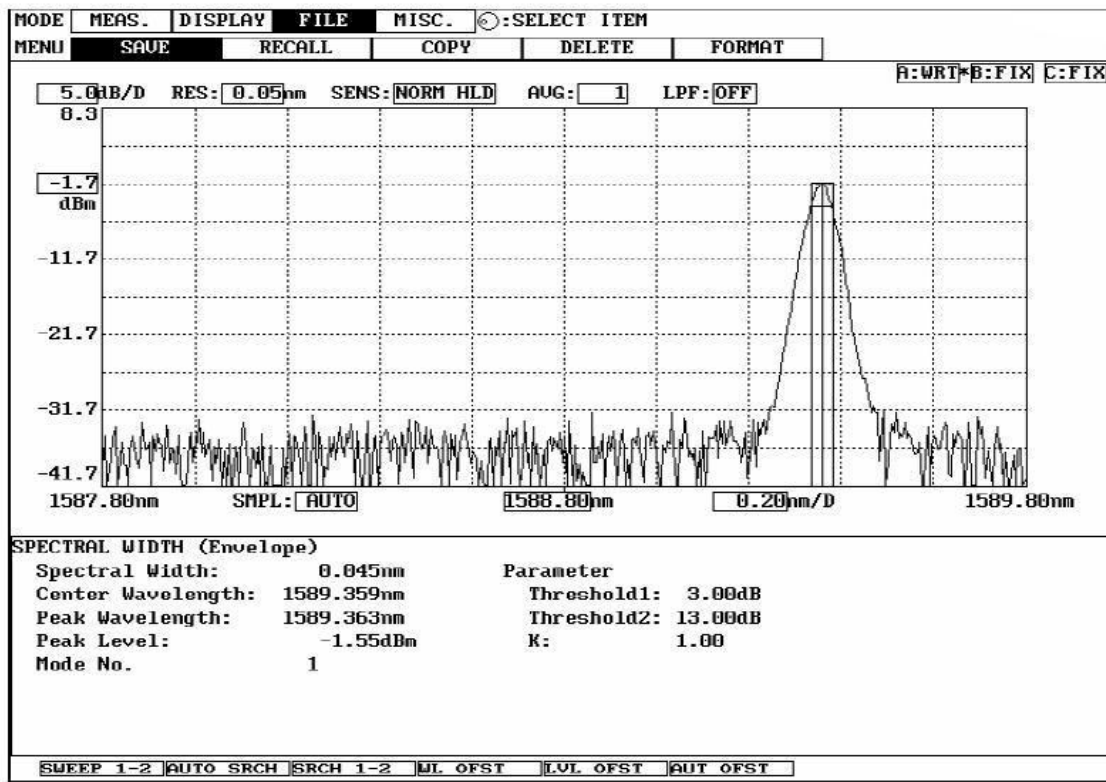


Fig. 25. Laser Spectrum at Voltage= 7 V

These figures show a tuning range of about 50 nm which varies from about 1540 nm to 1590 nm. This range is essentially defined by the tuning range of the tunable Fabry-Perot filter, and covers most of the wavelength range of C-band and L-band. In each case, the spectral width of the output is limited by the spectral resolution of the system; since, as mentioned earlier, the lasing wavelength peak seen in the display of the spectrum analyzer is actually a combination of a number of very narrow linewidth peaks. The effective tuning range of the ring laser system can easily be varied, according to the desired application, by choosing an appropriate filter.

As seen from the output spectrums, the tuning of this laser is quite linear. The operating wavelength dependence on applied DC voltage can be seen in Fig. 26. The graph is almost a straight line.

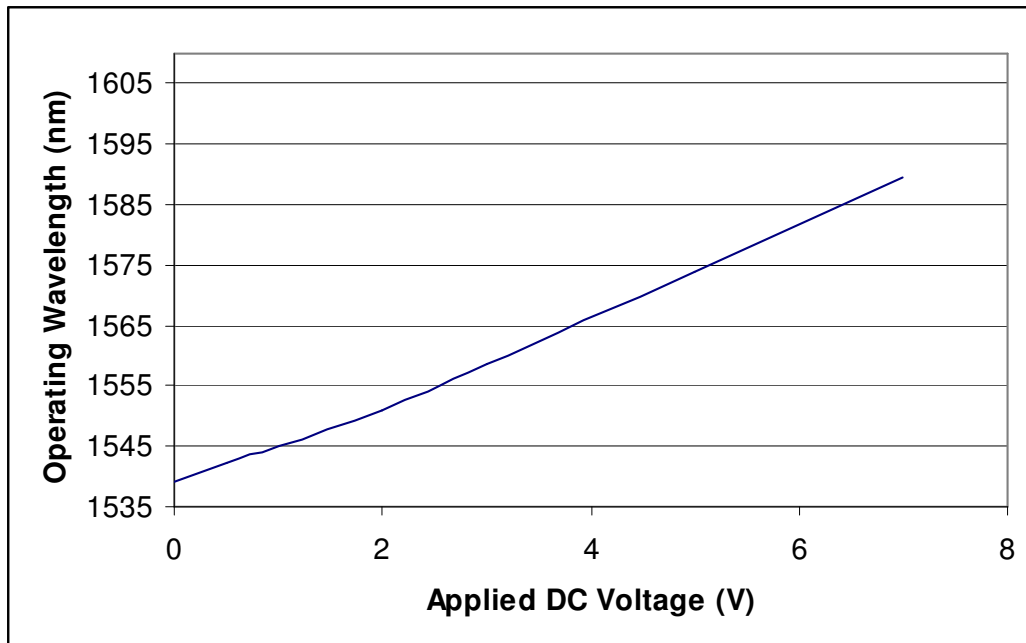


Fig. 26. Tuning – Wavelength vs. Applied Voltage

### C. Dynamic Tuning of Ring Laser

The terminals of the tunable Fabry-Perot filter are now connected to a function generator. The output of the signal generator is set to saw-tooth waveform with voltage varying from 0 V to 5 V. This signal can be applied at various frequencies. The output of the photodetector is connected to an oscilloscope. This directly shows us the degree of transmittance of the FFPI. The amount of light transmitted through the FFPI depends on the wavelength of the laser, which in turn is dependent on the applied voltage. The photocurrent produced by the photo detector is a function of the wavelength, and is given by

$$I = I_0(X + Y \cos \phi) \quad (6)$$

where  $I$  is the generated photocurrent,  $I_0$ ,  $X$ , and  $Y$  are constants, and  $\phi$  is the round-trip phase shift of the light in the interferometer. This  $\phi$  is in turn directly related to the length of the cavity, as mentioned earlier in Chapter II.

When the laser frequency is chirped linearly i.e. the optical frequency varies linearly with time, the photocurrent generated at the photodetector varies accordingly. An even and continuous change in the wavelength gives out a smooth change in the transmitted signal at the output of the FFPI. Similarly, a sudden shift or variation in the operation of laser will show up in the generated photocurrent.

The transmittance profile of the FFPI is given in the following figures.

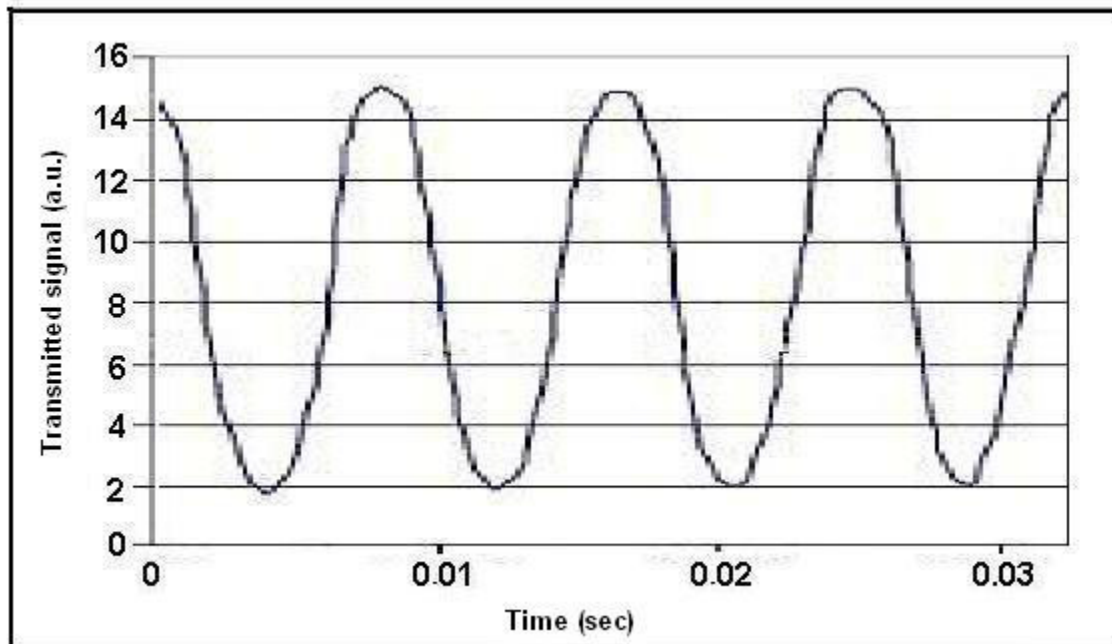


Fig. 27. FFPI Transmittance – 0.1 Hz

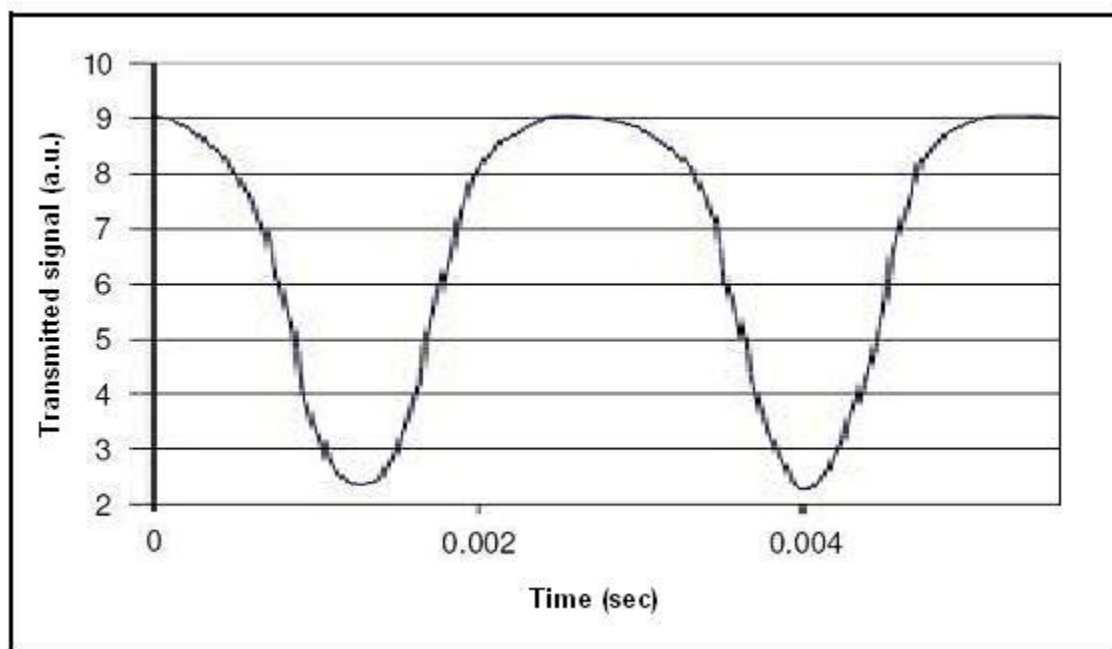


Fig. 28. FFPI Transmittance – 0.5 Hz

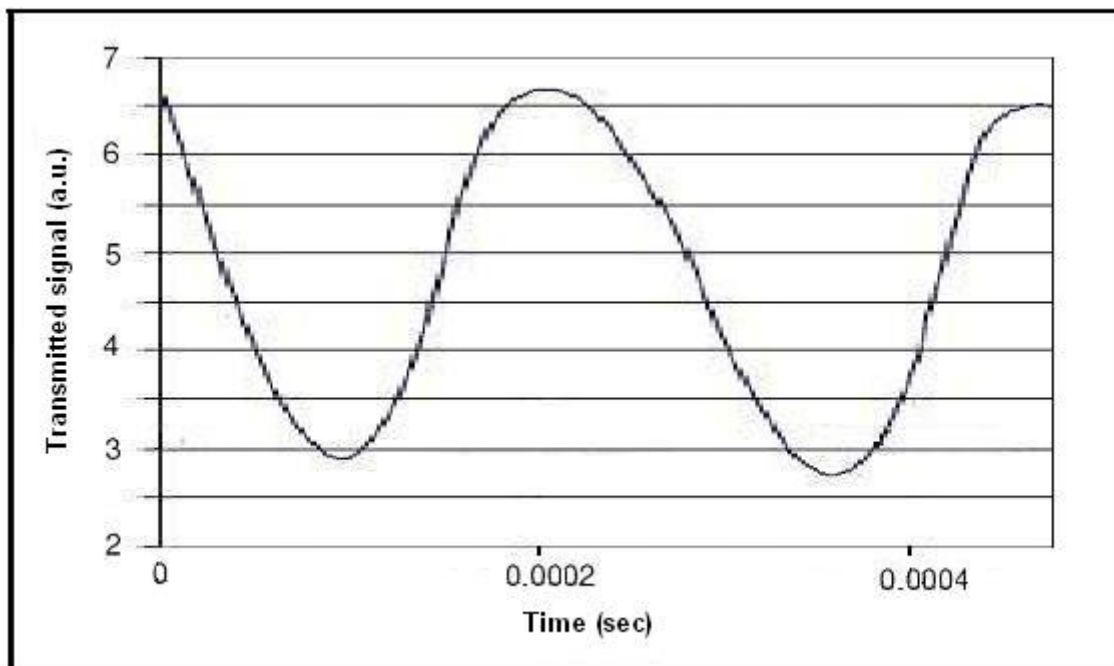


Fig. 29. FFPI Transmittance – 5 Hz

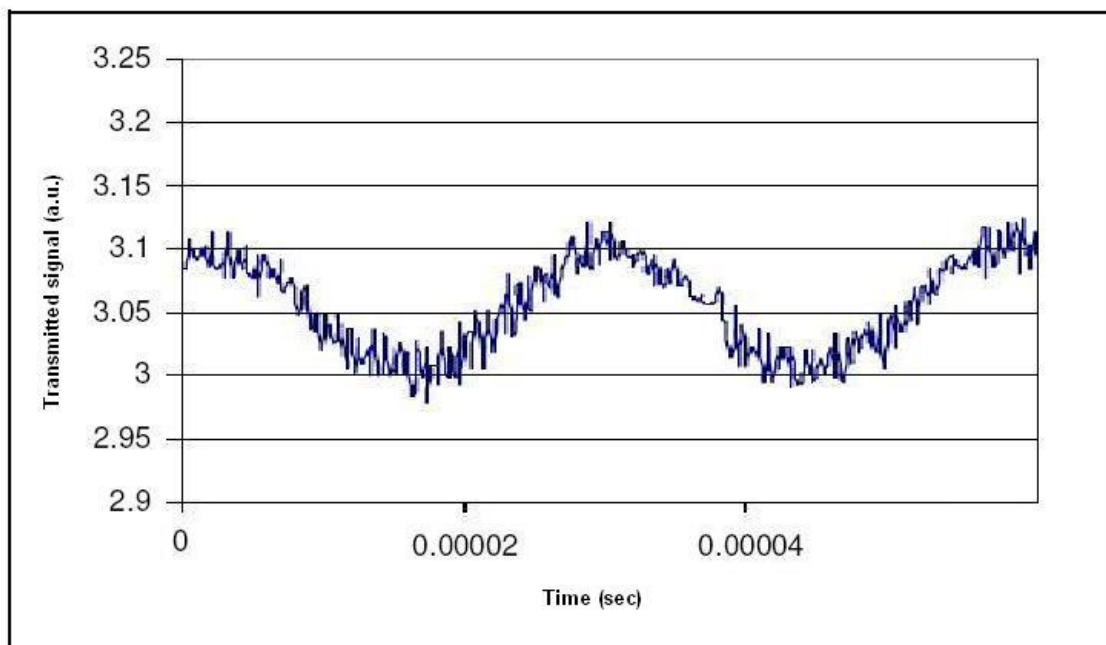


Fig. 30. FFPI Transmittance – 50 Hz

The graphs of Fig.28-30 show transmitted (or reflected signal) at various tuning frequencies. This data can be used to calculate the tuning speeds associated with corresponding tuning frequencies. As mentioned earlier from equation (3), the frequency change and phase shift of fringes are related. The change in frequency for every  $2\pi$  shift in the interferometer output is  $\lambda\nu/2nL$ . With refractive index of 1.458 and length of 1cm, the shift in frequency comes out to be 10.288 GHz, or in wavelength regime 0.082 nm. In Fig. 27, one complete fringe corresponds to 0.008 seconds. This means that the output wavelength shifts by 0.082 nm in 8 milliseconds. This corresponds to tuning speed of 10.25 nm/s. Similarly, tuning speeds related to rest of the tuning frequencies can be calculated. At frequency of 50 Hz, the tuning speed comes out to be 2733.33 nm/s.

An important characteristic associated with any interference related phenomenon is the fringe visibility. In almost all interferometers, interference manifests itself as oscillations in the output intensity. These are oscillations are called fringes. The interferometric visibility of these fringes, also termed as fringe visibility, is defined as

$$V = \frac{I_{\max} - I_{\min}}{I_{\max} + I_{\min}} \quad (7)$$

where  $I_{\max}$  and  $I_{\min}$  are the maximum and minimum of the output intensity, as shown in Fig. 31.

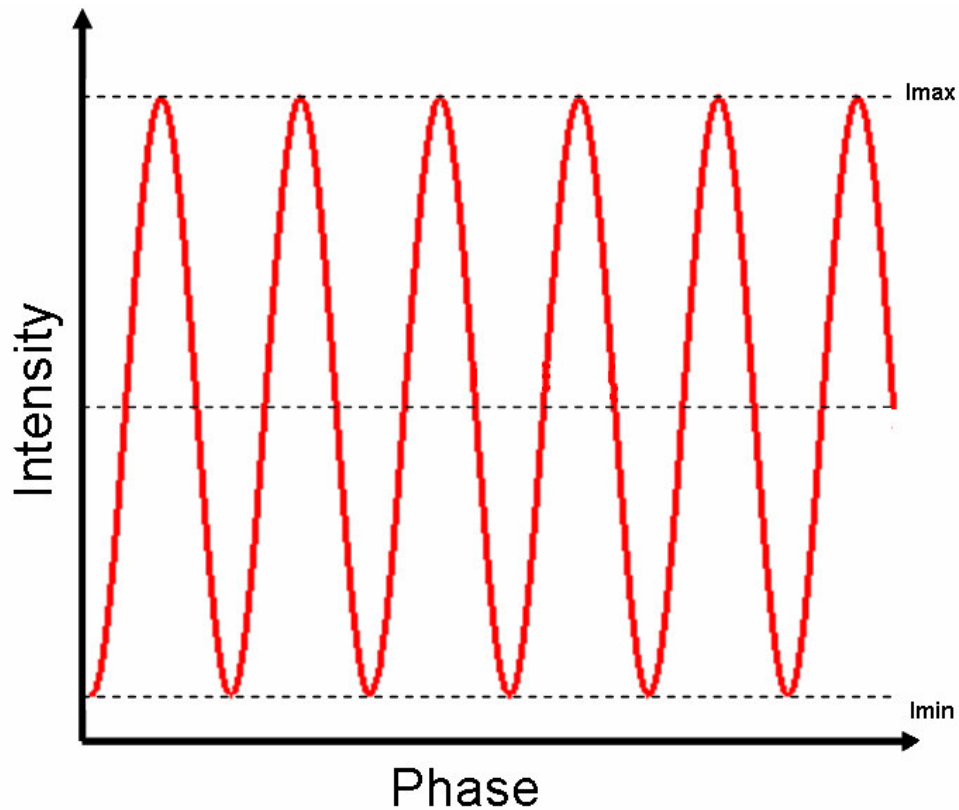


Fig. 31. Fringe Visibility

It is easily seen from the output of the photodetector that the fringe visibility decreases with increase in the tuning frequency. One of the reasons is that the extent of spectral broadening of the ring laser. The output fringe visibility pattern can be thought of as superposition of many individual patterns of narrow linewidth longitudinal modes. These individual patterns when combined create a low contrast visibility pattern. The higher the tuning frequency, greater is the degree of spectral broadening which in turn directly reduces the fringe visibility. The ring laser is unable to follow higher frequencies. This is a reason that a broadband source does not show any fringe visibility. The superposition of constituent wavelengths manifests itself as almost a straight line, or zero difference between maxima and minima in the transmittance profile of the interferometer.

Tuning of an erbium-doped fiber ring laser is essentially done by changing the effective gain profile of the system, with the help of the tunable filter. Hence the gain dynamics of erbium play a major role in putting an upper limit on such systems. The time dynamics of the gain process in an erbium-doped fiber laser give rise to transient effects. These effects can easily be seen when a non-steady state signal is being generated. The slow gain dynamics arise from the long excited-state lifetime of the erbium ions. The rather long stimulated lifetimes, which correspond to stimulated emission rates, also have an effect [15]. In this experiment, as the tuning frequency is increased, more and more modes of the ring laser cavity see the gain spectrum. In result, spectral broadening occurs while the power in individual modes decreases.



## CHAPTER V

### CONCLUSION

A tunable erbium-doped fiber ring laser has been experimentally demonstrated. Tuning is achieved by an intra-cavity voltage controlled Fabry-Perot filter. Static tuning characteristics have been studied by manually varying the applied DC voltage to the Fabry-Perot filter. To investigate the dynamic tuning characteristics, the filter is connected to a function generator set to saw-tooth waveform at different frequencies. The transmittance curves of fiber Fabry-Perot interferometer are used to examine the extent of spectral broadening of the ring laser system.

A 980 nm laser diode is used to pump the erbium-doped fiber. The threshold drive current is found out to be 37 mA. The slope efficiency is calculated to be about 0.07 mW/mA. Other components used in the setup include optical isolators, fiber couplers, and undoped single-mode fiber.

Static tuning of the system shows that the operating wavelength range of the system is from about 1540 nm to 1590 nm which covers most of the L-band in optical communications. The linewidth of the laser is essentially limited by the resolution of the optical spectrum analyzer, which is 0.05 nm.

Dynamic tuning characteristics are analyzed by observing the fringe visibility patterns of the fiber Fabry-Perot interferometer. A moderate tuning speed of 2733.33 nm/s has been demonstrated. The fringe contrast of the transmittance curves decreases with increase in the tuning frequency. At high tuning frequencies, gain dynamics of erbium-doped fiber are affected and transient effects come into play. The gain at a certain

wavelength becomes a function of time putting an upper limit on the tuning frequency of the system. The carrier lifetime of erbium ions dictates the maximum achievable tuning speed.

## **CHAPTER VI**

### **RECOMMENDATIONS**

The erbium-doped fiber ring laser system can be employed to a much larger range of wavelengths and is only limited by the range of gain spectrum of erbium ions. By choosing appropriate tunable filters, tuning wavelength can be shifted as per desired operation.

The length of the erbium-doped fiber length can affect the maximum tuning speed of the system. Tests can be done by employing various different lengths of erbium-doped fiber to investigate this particular effect. This will also influence the gain profile of the system.

## REFERENCES

- [1] E. Desurvire, J.R. Simpson, and P.C. Becker, "High gain erbium-doped traveling-wave fiber amplifier", *Opt. Lett.*, vol. 12, pp. 888-890, Nov. 1987.
- [2] M. C. Amann and J. Buus, *Tunable Laser Diodes*. Norwood, MA: Artech House, 1998.
- [3] Y. Kotaki and H. Ishikawa, "Wavelength tunable DFB and DBR lasers for coherent optical fibre communications", *IEE Proc. J*, vol. 138, pp. 171-177, Apr. 1991
- [4] P. Rigby.(2003, Jan). Tunable lasers revisited; Available:  
[http://www.lightreading.com/document.asp?doc\\_id=26332](http://www.lightreading.com/document.asp?doc_id=26332).
- [5] K. Kobayashi and I. Mito, "Single frequency and tunable laser diodes," *J. Lightwave Tech.*, vol. 6, pp. 1623-1633, Nov. 1988.
- [6] X. Wan, "The monitoring and multiplexing of fiber optic sensors using chirped laser sources," Ph.D. dissertation, Dept. of Elect. and Comp. Eng., Texas A&M University, College Station, 2003.
- [7] X. Wan and H. F. Taylor, "Linearly chirped erbium-doped fiber laser," *IEEE Photon. Tech. Lett.*, vol. 15, pp. 188-190, 2003.
- [8] H.J.R. Dutton, *Understanding Optical Communications*. Upper Saddle River, NJ: Prentice Hall PTR, 1998.
- [9] E. Hecht, *Optics*. San Francisco, CA: Addison Wesley, 2002.
- [10] J.C. Palais, *Fiber Optics Communications*. Upper Saddle River, NJ: Prentice Hall PTR, 1998

- [11] S.L. Hansen, K. Dybdal, and C.C. Larsen, "Upper gain limit in Er-doped fiber amplifiers due to internal Rayleigh backscattering," in *Proc. Opt. Fiber Commun. Conf.*, OFC'92, San Jose, CA, vol. 5, p. 68, 1992.
- [12] R.G. McKay, R.S. Vodhanel, R.E. Wagner, and R.I. Laming, "Influence of forward and backward traveling reflections on the gain and ASE spectrum of EDFA's," in *Proc. Opt. Fiber Comm. Conf.*, OFC'92, San Jose, CA, vol. 5, pp. 176-177, 1992.
- [13] P.C. Becker, N.A. Olsson, and J.R. Simpson, *Erbium Doped Fiber Amplifiers: Fundamentals and Technology*, San Diego, CA: Academic Press, 1999.
- [14] Yu, Francis T. S. and Yin, Shizhuo, *Fiber Optic Sensors*, New York: Marcel Dekker, Inc., 2002.
- [15] E Desurvire, "Analysis of transient gain Saturation and recovery in erbium-doped fiber amplifiers," *IEEE Phot. Tech. Lett.*, vol. 1, pp. 196-199, Aug. 1989.

## VITA

Bilal Hameed Malik was born in Karachi, Pakistan on January 13<sup>th</sup>, 1981. He received the Bachelor of Sciences degree in Engineering Sciences from the Ghulam Ishaq Khan Institute of Engineering Sciences and Technology in May of 2002.

After graduation, he continued his studies in the Department of Electrical Engineering at Texas A&M University under the direction of Dr. Henry F. Taylor and Dr. Chin B. Su. He worked as a Research Assistant from May 2004 to May 2006. He received his M.S. degree in electrical engineering in August 2006. His interests are in field of fiber optic communications and integrated optics.

Mailing Address: 214 Zachry Engineering Center  
3128 TAMU  
College Station, TX 77843-3128

The typist for this thesis was Bilal Hameed Malik